Elsevier Editorial System(tm) for Colloids and Surfaces A: Physicochemical and Engineering Aspects
Manuscript Draft

Manuscript Number:

Title: X-ray photoelectron spectroscopy investigation of nanoporous NiO electrodes sensitized with Erythrosine B

Article Type: SI: 30th ECIS Rome

Keywords: X-ray Photoelectron Spectroscopy
NiO
Erytrhosine B
Iodine

Corresponding Author: Dr. Matteo Bonomo,

Corresponding Author's Institution: La Sapienza

First Author: Matteo Bonomo

Order of Authors: Matteo Bonomo; Danilo Dini; Andrea G Marrani; Robertino Zanoni

Abstract: Nanoporous NiO thin films were prepared onto FTO glass substrates by means of screen-printing and were sensitized with Erythrosin B (EryB) dye. The obtained material was electrochemically treated and characterized with ex-situ X-ray photoelectron spectroscopy in order to gain information beneficial to the application of sensitized NiO as photocathodes of p-type dye-sensitised solar cells (p-DSCs). In particular, EryB-sensitised NiO films underwent a series of electrochemical treatments in LiClO4/Acetonitrile (ACN) electrolyte devised so as to simulate possible conditions the electrode might encounter during operation in the photoelectrochemical cell. Upon potential-cycling in a range where the two NiO faradic events Ni(II)□Ni(III) and Ni(III)□Ni(IV) occur, X-ray photoelectron spectroscopy revealed that Erythrosin B dye experiences a partial detachment from the NiO surface. This detachment seems to be paralleled by the formation of stable (Ni)+(ClO4)- couples. Overall, the EryB dye displayed an acceptable electrochemical stability onto the surface of NiO electrode up to 50 cyclic voltammetries in the range -0.27 ÷ +1.13 V vs. Ag/AgCl. These results are useful for the evaluation of electrochemical stability of the dye when the this is immobilised onto an electrode surface and are beneficial for a better comprehension of the degradation phenomena operating in real photoconversion device.

Cover Letter

Università degli Studi "La Sapienza"di Roma

DIPARTIMENTO DI CHIMICA

Prof. Danilo Dini
Tel.: -39-06-4991 3335
Fax: -39-06-490324
e-mail: danilo.dini@uniroma1.it

Rome , 27th Feb 2017

Dear Editor,

the manuscript we intend to submit for consideration of publication in the special issue of Surface and Colloids A (dedicated to the contributions of the ECIS 2016 conference held in Rome during September 2016) reports the detailed analysis of the electroactivity of nanostructured electrodes of nickel oxide (NiO) sensitized with Erythrosine B (EryB) undergoing simultaneous chemical and electrochemical processes in organic electrolytes when the electrode is polarized. The procedures of NiO synthesis and its deposition as thin film have been originally developed by our research group. Electrodes undergone electrochemical treatment were analyzed by X-ray Photoelectron Spectroscopy (XPS) in order to gain information beneficial to their application as electrodes in p-type dye-sensitised solar cells (pDSCs). In particular, Cyclic voltammetry showed that the NiO surface is not completely electrically passivated by the adsorbed dye . XP spectra revealed that the EryB dye experiences a partial detachment from the NiO surface. This detachment seems to be followed by the formation of stable $(Ni)^{+}(ClO_4)^{-}$ couples, which leads to an increase of Cl species signals parallel to the decrease of EryB peaks. Overall, the EryB-sensitized electrodes displayed an acceptable electrochemical stability up to 50 cyclic voltammetries in the range -0.27 ÷ +1.13 V vs. Ag/AgCl.
For these reasons we believe that the content of the present work fits with the aims of this journal, and can attract the interest of a broad audience ranging from surface scientists, materials scientists, inorganic chemists and electrochemists who are involved in the preparation, characterization and applications of semiconducting electrodes.
Thank you for the consideration.

Best regards,

Danilo Dini

*Graphical Abstract (for review)

TOC graphics

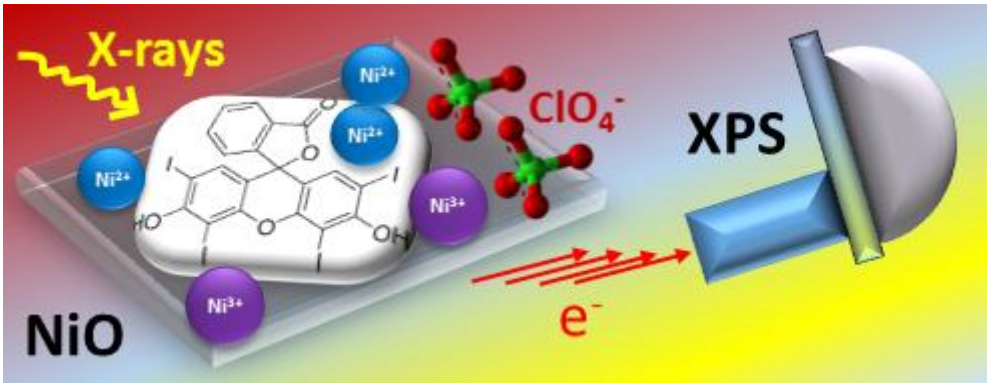

***Highlights (for review)**

- Electroactive NiO films are deposited via screen printing with NiO nanoparticles

- Screen-printed NiO is mesoporous

- Screen-printed NiO films are conducting and make a good electrical contact with the substrate

- NiO electrode are sensitized with Erythrosine B

- X-ray Photoelectron Spectroscopy analysis reveal a partial desorption of Erythrosine during electrochemical treatment

- NiO surface is not completely electrically passivated by the adsorbed dye

- The Erythrosine dye displayed an acceptable stability onto the surface of NiO electrode

X-ray photoelectron spectroscopy investigation of nanoporous NiO electrodes sensitized with Erythrosine B

Matteo Bonomo, Danilo Dini, Andrea Giacomo Marrani*, Robertino Zanoni

Department of Chemistry, University of Rome "La Sapienza", P.le Aldo Moro 5, 00185 Rome, Italy

*Corresponding author. Tel.: +39 06 4991 3344; fax: +39 06 49913175.

E-mail address: andrea.marrani@uniroma1.it

Abstract

Nanoporous NiO thin films were prepared onto FTO glass substrates by means of screen-printing and were sensitized with Erythrosin B (EryB) dye. The obtained material was electrochemically treated and characterized with *ex-situ* X-ray photoelectron spectroscopy in order to gain information beneficial to the application of sensitized NiO as photocathodes of *p*-type dye-sensitised solar cells (*p*-DSCs). In particular, EryB-sensitised NiO films underwent a series of electrochemical treatments in $LiClO_4$/Acetonitrile (ACN) electrolyte devised so as to simulate possible conditions the electrode might encounter during operation in the photoelectrochemical cell. Upon potential-cycling in a range where the two NiO faradic events Ni(II)→Ni(III) and Ni(III)→Ni(IV) occur, X-ray photoelectron spectroscopy revealed that Erythrosin B dye experiences a partial detachment from the NiO surface. This detachment seems to be paralleled by the formation of stable $(Ni)^{+}(ClO_4)^{-}$ couples. Overall, the EryB dye displayed an acceptable electrochemical stability onto the surface of NiO electrode up to 50 cyclic voltammetries in the range -0.27 ÷ +1.13 V vs. Ag/AgCl. These results are useful for the evaluation of electrochemical stability of the dye when the this is immobilised onto an electrode surface and are beneficial for a better comprehension of the degradation phenomena operating in real photoconversion device.

1. Introduction

With the advent of the dye-senstized solar cell in 1991 [1], the interest towards the electronic structure of nanostructured semiconductors[2] and their properties in the dye-sensitized state[3] has received a strong stimulus especially in the direction of electrochemistry[4] and photoelectrochemistry[5–7]. Among the various typologies of DSCs based on nanostructured electrode the most performing ones are the solar conversion devices of *n*-type which can reach conversion efficiencies as high as 14 %[8], whereas the analogous *p*-type version represents the poorest DSC configuration since it achieves efficiencies typically inferior to 5 %[9]. For this reason the researchers have directed their efforts towards the development of more performing *p*-DSCs with the final goal of attaining tandem devices (*t*-DSCs), i.e. the photoelectrochemical cells having both electrodes photoelectrochemically active[10–13], which present the highest theoretical efficiency[14], with the maximum achievable level of transport current.

In the general perspective of ameliorating the performance of *p*-DSCs several approaches have been adopted, e.g. the variation of the photoelectrodic material, the nature of the dye-senstizer or the chemical composition of the electrolyte[4,7]. In the framework of our research focussed on *p*-DSCs we were mostly interested to the preparation and characterization of NiO cathodes with open and nanostructured morphology[15–19]. Among the major advantages of NiO there is the possibility of producing it as a transparent thin film when $l < 3$ μm, with electrical conductivity and optical transmission controllable by means of electrical fields, chemical/electrochemical doping[20] or irradiation in the UV-visible spectrum[21]. In the present work, we aim at elucidating the surface electronic structure of the mesoporous NiO thin films obtained via screen-printing[16] with the technique of XPS[22] when these films are sensitized with Eritrhosine B (EryB), a typical benchmark dye for NiO based *p*-DSCs[15,18,23–26], and are polarized at different redox states in non aqueous electrolytes.

2. Experimental

Preparation of screen-printing paste

The viscous paste utilized as precursor for the screen-printing deposition of NiO has been prepared according to the procedure of Bonomo *et al.*[27]. All chemicals here employed were purchased from Sigma-Aldrich or Fluka at the highest degree of available purity and were used without any further purification.

2.1 NiO film deposition

Mesoscopic NiO photocathodes were obtained via screen-printing of a slurry containing preformed NiO nanoparticles (diameter, $Ø \leq 50$ nm). NiO nanoparticles were grinded with 5 mL of water and 30 mL of ethanol. Then 20 mL of terpineol and 30 g of ethylcellulose (10% w/w in ethanol solution) were added to enhance the viscosity of the paste. The resulting paste was deposited onto FTO-coated glass with a manual screen-printer and a square viscous coating with area 0.5 cm^2 was obtained. The electrodes were then sintered in oven at 450 °C for 30 minutes[16]. The electrodes were successively sensitized by dipping in a 0.2 mM solution of Erythrosin-B in ethanol for 16h. After sensitization they were rinsed with pure ethanol in order to remove the molecules of dye which were not chemisorbed onto NiO surface.

2.2 Electrochemical characterization of NiO electrodes

The electrochemical properties of Erythrosine B-sensitized NiO thin films (EryB/NiO) were studied with a three-electrode cell configuration: EryB/NiO-covered FTO was the working electrode, a Pt wire was the counter electrode, and Ag/AgCl was used as reference electrode. The electrolyte was 0.2 M $LiClO_4$ in acetonitrile (ACN). The applied potential values here reported are all referred to the Ag/AgCl electrode (*E vs.* NHE = 0.21 V). Prior to XPS analysis, NiO electrodes underwent different electrochemical treatments: (i) cyclic voltammetry (1, 25 and 50 cycles) at a scan rate of

0.01 V s^{-1} between -0.27 and 1.13 V *vs.* Ag/AgCl, with initial and end potentials corresponding to the open circuit potential (OCV) (samples denominated **CV1, CV25** and **CV50**, respectively in the case of 1, 25 and 50 voltammetric cycles); (ii) chronoamperometry at E_{appl} = 0.9 V (this value corresponds to the electrical potential generating the second oxidation wave of pristine NiO, *vide infra*) with a step duration of 5000 s. The sample thus polarized was denominated **ox**; (iii) cyclic voltammetry (1 cycle) at a scan rate of 0.01 V/s from OCV to 1.13 V and back to -0.27 V followed by a reducing chronoamperometry at -0.27 V for 5000 s (sample here denominated **red**). As references, two different samples were analyzed by XPS. One was a EryB/NiO electrode prior to any electrochemical treatment (called **pristine**); another one was a graphite foil wet by few drops of the 0.2 mM solution of EryB (called **graphite**). This latter sample was devised in order to better discern in the spectra possible contributions deriving from chemical interaction between EryB and the surface of NiO. Cyclic voltammetries and chronoamperometric curves were recorded with the potentiostat/galvanostat Autolab PGSTAT 128N, and analyzed with the software NOVA 1.9. After electrochemical experiments the NiO electrodes were thoroughly rinsed with pure ACN and dried with a stream of nitrogen. All the samples were mounted onto the XPS sample holder with an adhesive scotch tape and a drop of silver paste to ensure electrical contact. Sample introduction in the XPS load lock chamber was made as quick as possible to avoid eventual surface contamination from ambient atmosphere.

2.3 X-ray photoelectron spectroscopy

XPS measurements were performed with a modified Omicron NanoTechnology MXPS system equipped with a dual X-ray anode (Omicron DAR 400) and an Omicron EA-127 7-channeltron energy analyzer. XP spectra were acquired using Mg Kα photons (hν = 1253.6 eV) as excitation source, generated with the anode operating at 14 kV and 14 mA. No charging was experienced during measurements. For all the samples the spectral regions associated with the ionization of Ni 2p, I 3d, I 4d, O 1s, C 1s, Cl 2p levels were acquired using an analyzer pass energy of 20 eV. A

survey scan at 50 eV of pass energy was also taken. A take-off angle (θ) of 21° with respect to the direction normal to the surface was considered. The measurements were performed at room temperature and the base pressure in the analyzer chamber was about 2×10^{-9} mbar during the recording of the spectra. The binding energy (BE) of the Ni $2p_{3/2}$ peak at 854.0 eV, associated to the $\underline{c}d^9\underline{L}$ final state configuration in NiO [28], was used as an internal standard reference for scaling the BE (accuracy of ±0.05 eV). The experimental spectra were theoretically reconstructed by fitting the secondary electrons background with a linear or a Shirley function (subtracted from the experimental spectrum after optimization), and the elastic peaks with symmetric pseudo-Voigt functions described by a common set of parameters (position, FWHM and Gaussian-Lorentzian ratio) free to vary within narrow limits. The Gaussian-Lorentzian ratio varied between 0.7 and 0.8. XPS atomic ratios between relevant element components were estimated from experimentally determined area ratios (with ±10% as associated error), which were corrected for the corresponding photoelectron cross sections according to Scofield calculations [29], and for the square root dependence of the photoelectrons kinetic energy.

2.4 Electron microscopy

Morphological investigation of NiO thin films was performed using a field-emission scanning electron microscope (FE-SEM) Zeiss Auriga 405 (c/o SNN-Lab−Sapienza Nanoscience & Nanotechnology Lab).

3. Results and discussion

3.1 Electrochemical features of EryB/NiO electrodes

Figure 1 shows the evolution of the voltammogram of EryB sensitized NiO when this is immersed in a non aquesous electrolyte. The current profiles recall the typical ones of NiO in the sensitized state when the dye-sensitizer is not electroactive within the range of NiO oxidation[17,22,24,30]. The novel aspect of this series of data is represented by the verification of

sensitizer detachment upon continuous cycling of NiO even if the dye in question (EryB) is not electrochemically active. As a confirmation of that, there is no evidence of redox peaks associated to EryB based processes within the potential range here examined (Figure 1). In fact, the presence of EryB induces a process of NiO electrode passivation as previously verified when the voltammograms of bare and EryB sensitized NiO were compared under the same experimental conditions[17]. In the present case the continuous cycling of potential leads to an increase of the amplitude of the current density exchanged reversibly by EryB sensitized NiO during its oxidation (Figure 1, bottom frame). These findings indicate a progressive detachment of EryB upon repetitive oxidation of sensitized NiO electrode with the consequent appearance of the electrochemical features typical of bare NiO after about 200 full cycles. Figure 2 presents the chronoamperometric curves of EryB sensitized NiO when the electrode is brought to the fully polarized state at 0.9 V *vs* Ag/AgCl and to the neutral state at -0.27 V *vs* Ag/AgCl. These two electrochemical processes occur in the solid state[22] and display a different kinetics since oxidation of NiO is not completed at the end of the time window of 5000 s whereas the electrochemical neutralization of NiO is fully achieved within the same temporal range (Figure 2).

3.2 XPS analysis of EryB/NiO electrodes

X-ray photoelectron spectroscopy was used in order to investigate the nature of molecular species adsorbed onto the NiO porous thin films, such as the dye EryB and the supporting electrolyte $LiClO_4$, and to follow the possible variation of their relative concentration along the different electrochemical treatments applied to the modified electrode. Such treatments were introduced in order to simulate the possible conditions the electrode may encounter within a real p-type dye-sensitised solar cell (*p*-DSC) during operation, and have been devised both to test the stability of the EryB dye and to investigate the possible adsorption of perchlorate anions onto the surface of NiO. To these aims, the XPS technique was chosen due to its unparalleled chemical environment and

oxidation state sensitivity, as well as its surface sensitivity. The most relevant photoionization regions reported in this work are those related to the iodine atoms of the EryB dye, in particular the I 4d and I 3d regions, and those associated to the chlorine atoms in perchlorate electrolyte, i.e. the Cl 2p region.

I 4d.

Figure 3 shows the I 4d XP spectra of the EryB/NiO electrodes prior (b) and after (c – g) being used as a working electrode in a three-electrode cell in the presence of a $LiClO_4$/ACN electrolyte. The spectrum of EryB over graphite (a) is also reported as a further spectroscopical reference. To our knowledge, the following results are the first obtained with XPS applied to the EryB dye.

Photoionization of the I 4d level in iodine compounds is significantly more explored in the literature than that of the higher cross-section I 3d orbital. The reason is probably that I 4d photoionization cross-section results markedly enhanced upon shape-resonance conditions, when tunable photon sources are used [31]. Furthermore, the energy of I 4d orbital is probably more sensitive to changes in the chemical environment compared to I 3d, see for example the too small BE differences found in iodide (I^-) and triiodide (I_3^-) species for this latter orbital [32,33] compared to the former [34–36]. We recently reported on the XP spectral features of I^- and I_3^- in the I 4d region [36], and, in order to allow for a systematic comparison between those species and the iodinated dye reported here, we will start commenting on I 4d features.

Spectra (a) and (b) of Figure 3, denominated **graphite** and **pristine** were respectively recorded from a graphite and a NiO sample dipped in EryB ethanolic solution without any implementation in an electrochemical cell, in order to constitute reference data for the interpretation of the forthcoming samples. Both spectra display one spin-orbit split doublet (j = 5/2, 3/2 for d-type orbitals, with branching ratio close to 1.5) whose components are separated by 1.7 eV [34,37–40]. These doublets, whose j = 5/2 part falls at a 50.15 eV BE, are attributed to the four iodine atoms in EryB, approximately considered chemically equivalent (the formal non-equivalence due to long-

range interactions with hydroxyl and ethereal O atoms, reasonably leading to a very small chemical shift, could not be discerned). The BE values found for the I 4d spectral features of EryB are more positive than those found previously by us for I^- and I_3^- species [36], which we reported to fall around 48 eV. This chemical shift can be explained with a simple electrostatic argument, i.e. the most easily ionisable iodinated system is that of I^- anion, which bears the highest negative charge density on I atom, hence displaying the lowest BE. On the other hand, I atoms in EryB molecule are covalently bound to C atoms, therefore experiencing a minor fraction of negative charge, which increases their BE compared to I^-. The choice of graphite as a substrate for adsorption of EryB dye was directed by the need for a seemingly inert matrix which would possibly allow to discern the spectral features of the dye as non-interacting moiety. This would eventually permit to attribute the possible differences found once the dye is adsorbed onto the NiO film to its interaction with the NiO itself. By looking at spectrum (b) of Figure 3, i.e. the **pristine** Ery/NiO sample, no differences can be found with the **graphite** sample. This definitely rules out the possibility of discerning, if any, the interaction features of I atoms of EryB dye with the NiO film.

The following I 4d spectra, from (c) to (f) all display the same doublet, whose BE value oscillates between 50.0 and 50.2 eV and full width at half maxima (FWHM) between 1.35 and 1.45 eV, which demonstrates that the dye remains substantially unaltered along the electrochemical treatments it is subject to. What is evident, instead, is the nearly total absence of I 4d signal in spectrum (g), related to the **CV50** sample, i.e. the EryB/NiO electrode subject to 50 voltammetric cycles. This dye depletion already starts in the **red** sample (spectrum (c)). In fact, as reported in Table 1, the amount of EryB molecule adsorbed onto NiO, as calculated by the ratio between the areas of I $3d_{5/2}$ and Ni $2p_{3/2}$ peaks (see Experimental Section for details), was found to decrease from the **pristine** to the once-cycled **CV1** sample, and again dramatically to the other samples (**CV25**, **red** and **ox**), ending in a nearly total absence in **CV50** sample (classified as non-detectable in Table 1). This trend suggests that prolonged electrochemical treatments, like chronoamperometric (both at reductive and oxidative potentials) and repeated cyclic potential

scanning experiments, are likely to induce detachment of a fraction of molecules. This depletion was found to be more important in the case of repeated potential cycling, as displayed by the results from the **CV50** sample compared to those from the samples undergoing chronoamperometric experiments (**red** and **ox**). The decrease of I signal after electrochemical treatments, likely associated to detachment of EryB dye from the NiO electrode, is coherent with the results from the electrochemical tests themselves. In fact, as evident in Figure 1 and described above, upon repeated potential cycling an increase of faradic current was recorded, associated to an increase in the number electroactive Ni^{2+} and Ni^{3+} sites, which probably become more and more available to charge transfer as the EryB dye gets detached along potential cycling.

I 3d.

Figure 4 reports the I 3d photoionization region for all the samples investigated. As mentioned above, I 3d is the orbital with the highest photoionization cross-section for I atom, but probably the less useful when species like I^- and I_3^- have to be detected and monitored [36]. In our case, I 3d area was used for determining the relative amounts of EryB adsorbed onto the different samples, relative to the most intense Ni 2p signal in NiO (see Table 1). Furthermore, the BE position of I 3d doublet was evaluated in order to possibly confirm the assignment done on the basis of I 4d analysis. The I 3d spectra appear as well resolved spin-orbit split doublets (ΔE_{so} = 11.4 eV) with a symmetrical shape (except for Mg Kα ghost lines)[40]. The $3d_{5/2}$ component falls around 620.50 eV BE, which is significantly higher than those associated to I^- and I_3^- species reported in our previous work [36], thus confirming that this chemical shift can be associated to the I-C bond in EryB molecule [41–44]. As also shown by the I 4d spectra, no sizeable position shift can be detected among the different samples, but only an intensity variation. In particular, the most suppressed signal is confirmed to be that of CV50 sample (spectrum (g)), where no fitting reconstruction was attempted due to low signal-to-noise ratio. One additional feature of I 3d spectra compared to I 4d ones is the appearance of a doublet shoulder at lower BE than the main contribution in spectra (b) to (f). This

minor doublet is located ~2 eV lower than the main one, and is probably due to degradation of EryB dye upon prolonged X-ray exposure. Its occurrence is limited to I 3d signals since these were always acquired after the I 4d region, thus after longer X-ray exposures.

Cl 2p.

The Cl 2p XP spectra were recorded in order to monitor the amount and possible modifications of ClO_4^- anions adsorbed onto the nanoporous NiO film coming from the electrolytic solution used for electrochemical measurements. Figure 5 shows the Cl 2p region of sample **ox** and is separated in two panels ((a) and (b)) representing the Cl 2p region for the same sample within the same measurement run, but recorded at different times (t = 0 and t = 1 h, respectively), thus experiencing different X-ray exposures. Therefore, the apparent complexity of the peaks envelope derives from degradation of perchlorate (ClO_4^-, red peak) under X-ray beam and its transformation into lower oxidation state iodine compounds, such as chlorate (ClO_3^-, green peak) and chloride (Cl^-, blue peak). The Cl 2p photoionization signal is displayed as a narrow spin-orbit split doublet with a 3/2-1/2 separation of 1.6 eV. The ClO_4^- contribution displays a strong chemical shift due to the high oxidation state of Cl atom and falls at 207.90 eV (3/2 component) [45,22]. As the oxidation state decreases, so does the BE of the associated Cl species. Therefore, ClO_3^- is found at 205.80 eV [45], while Cl- at 197.90 eV [40,46]. In all the samples investigated the Cl 2p signals were found to evolve during X-ray exposure, and as reported in Figure 5 for sample **ox**, an intensity increase of the lower oxidation state Cl species was detected at the expenses of ClO_4^- contribution on going from t = 0 to t = 1 h. It is worth mentioning that the area of the overall Cl 2p ionization envelope remains constant throughout the acquisition time of the XP spectrum. The relative amount of adsorbed Cl species onto the NiO surface was determined by means of XPS and the corresponding data reported in Table 1. Perchlorate anions act as electro-inactive supporting electrolyte in the solution for electrochemical tests, with the sole scope of ensuring good electrical conductivity and avoid migration overvoltage. On the other hand, as already reported by us recently [22], ClO_4^-

anions act as charge-balancing agents with respect to the positively charged Ni(III) and Ni(IV) sites generated in-situ during potential scanning in the anodic direction. Therefore, their concentration as adsorbed species onto the porous NiO surface is expected to vary in function of the electrochemical treatment applied to the electrode itself. In fact, what we found is that the Cl/Ni ratio, as determined by the area ratio of Cl 2p and Ni $2p_{3/2}$ signals (see Experimental Section for details), increases dramatically on going from the **pristine** sample (which, in this case, was immersed in the electrolytic solution for 1 min) to sample **ox** (see Table 1). In order to account for the significantly increased presence of perchlorate anions after the oxidative treatment, one has to consider the redox behaviour of NiO. Electroactivity of bare NiO has been already reported both in aqueous and organic electrolytes [28,22,17,47–49], resulting in two reversible redox events associated to formal oxidation of Ni^{2+} centers to Ni^{3+} and Ni^{4+}. As mentioned in the Electrochemical Section, in acetonitrile the two oxidation steps occur within the +0.9 V upper limit, hence according to the results from XPS it is reasonable to associate the presence of ClO_4^- signal to an electrostatically driven adsorption of ions inside the NiO pores upon formation of Ni^{3+} and Ni^{4+} sites. Furthermore, XP spectra in the I 4d and 3d regions revealed that the prolonged oxidative treatment provokes a sizeable detachment of dye molecules, likely leaving even more Ni sites available for interaction with perchlorate. On the other hand, the amount of Cl species detected at the surface of NiO after prolonged reductive polarization (sample **red**) was found to decrease below the untreated pristine sample. The adsorption of anions onto the surface of **pristine** NiO is due to the presence of Ni^{3+} sites, naturally embedded as defects in the non-stoichiometric NiO framework. Upon reduction at -0.27 V, these sites are partially converted to Ni^{2+} sites and the electrode itself is negatively polarized. These conditions of polarization should prevent the spontaneous adsorption of negatively charged perchlorate. As to the effect of one single voltammetric cycle (sample **CV1**), no variations are found compared to the **pristine** sample, whereas an increase of anion adsorption is detected upon increasing the number of CV cycles (samples **CV25** and **CV50**), parallel to the abatement of

EryB signal. This trend calls for a gradual increase of stabilized $(Ni)^{+}(ClO4)^{-}$ couples due to partial detachment of EryB dye molecules.

Ni 2p and survey spectra.

In Figure 6, the survey spectrum of the **pristine** sample is reported as an indicative example of the overall elemental composition of all the samples investigated in this work. The most intense photoemission and Auger peaks related to the EryB/NiO system can be identified (Ni 2p, Ni LMM, O 1s, O KVV, I 3d, C 1s) together with minor contributions from Sn due to possible microscopic scratches exposing the underneath surface of FTO glass substrate to the X-ray beam. In the inset of Figure 6, a high-resolution XP spectrum of Ni 2p region is reported, revealing the typical envelope of NiO [50–53]. A thorough description of the bare NiO XP spectral features can be found in previous works by us and other authors [28,50,52,53]. In particular, the Ni $2p_{3/2}$ region appears complicated due to interaction between different electronic configurations in the final state after the creation of the 2p core-hole upon photoemission. The corresponding six peaks deriving from such interaction unfold in the range 850-870 eV, the first one being attributed to the $\underline{c}d^{9}\underline{L}$ state ($\underline{c}$ and $\underline{L}$ respectively represent holes in the 2p level and in a ligand orbital) [52,54], and originating from an on-site charge transfer (CT) process between the O^{2-} ligands and the central Ni cation, with the latter representing the locus where the core-hole resides. This peak falls at 854.0 eV and in this work has been chosen as reference for BE scale calibration. As to the other contributions to the overall Ni 2p envelope, we indicate here those appearing as a shoulder to the first peak mentioned above, unfolding in the range 855-860 eV. These two signals are associated to core-hole screening processes occurring at the surface, where the bulk symmetry is reduced and the coordination geometry around Ni is lowered from the octahedral NiO_6 to the square-pyramidal NiO_5 [51,53,55]. These signals have been reported to be diagnostic of surface-confined relaxation processes [51,55–58], and in many cases, have been naively associated to the presence of Ni^{3+} defects [59,60]. Although NiO is undoubtedly an off-stoichiometric compound with Ni^{3+} defects, during the years it

has been widely accepted [54,61] that recognition of a Ni^{3+} feature within the Ni 2p photoionization envelope cannot be operated unless a genuine Ni(III) compound is actually under consideration, such as NiOOH [28,62]. The substantial similarity found among the Ni 2p spectra (not shown) of all the investigated samples confirms that in non-aqueous electrolytes the Ni 2p XPS region results substantially insensitive to electrogenerated Ni(III) and Ni(IV) centres.

Conclusions

Nanoporous NiO thin films were deposited onto FTO glass substrates by means of screen-printing technique followed by sensitization with Erythrosin B dye. The obtained material has been characterized by means of electrochemical methods followed by ex-situ X-ray photoelectron spectroscopy in order to gain information beneficial to their application as electrodes in p-type dye-sensitised solar cells (pDSCs). The sensitised EryB/NiO system underwent an experimental protocol devised so as to simulate possible conditions the electrode might encounter during operation within a real pDSC device. Therefore, oxidative, reductive and potential-scanning treatments were applied via utilization of said electrode in a three-electrode cell in the presence of the $LiClO_4$/ACN electrolyte. Cyclic voltammetry showed that the NiO surface is not electrically passivated by the adsorbed dye, therefore, the two corresponding faradic events Ni(II)→Ni(III) and Ni(III)→Ni(IV) are well visible. Moreover, as the number of cycles increases, the current density of said processes increases, along with a sizeable peak potential shift towards cathodic values. XP spectra revealed that the EryB dye experiences a partial detachment from the NiO surface already at the 25^{th} CV cycle, while it is found to disappear almost completely at the 50^{th} cycle. This detachment seems to be followed by the formation of stable $(Ni)^{+}(ClO_4)^{-}$ couples, which leads to an increase of Cl species signals parallel to the decrease of EryB peaks (except for the case of the negatively polarized sample). Also the oxidative and reductive prolonged polarizations are found to be detrimental with respect to amount of adsorbed dye, although their effects seem to be

comparable to that of potential-scanning up to the 25th cycle. Overall, the EryB dye displayed an acceptable stability onto the surface of NiO electrode only within a potential-scanning protocol limited to no more than 50 cycles in the -0.27 ÷ +1.13 V vs. Ag/AgCl, wherein the two redox processes of NiO surface are expected to occur. In the context of the suitability of EryB sensitized NiO as photocathodes of *p*-DSCs, these results bear a great importance since the electrochemical injection of holes in EryB sensitized NiO is equivalent to the dye-mediated injection of holes in the same sample under irradiation. The results presented here have demonstrated that the electrochemical injection of holes in EryB sensitised NiO brings about the detachment of the electrode even though the dye does not get directly oxidized. This phenomenon of desensitization is quite anomalous for such a type of systems because hole-induced detachment of sensitizer was previously verified only with squaraines that undergo a direct process of oxidation when holes are electrochemically injected in NiO.

Acknowledgements

D.D. acknowledges the financial support from the University of Rome "LA SAPIENZA" through the programs Ateneo 2012 (Protocol No. C26A124AXX) and Ateneo 2016.

References

[1] B. O'Regan, M. Gratzel, A low-cost, high-efficiency solar cell based on dye-sensitized colloidal TiO2 films, Nature. 353 (1991) 737.

[2] A. Hagfeld, M. Grätzel, Light-induced redox reactions in nanocrystalline systems, Chem. Rev. 95 (1995) 49.

[3] H. Gerischer, M.E. Michel-Beyerle, F. Rebentrost, H. Tributsch, Sensitization of charge injection into semiconductors with large band gap, Electrochim. Acta. 13 (1968) 1509. doi:10.1016/0013-4686(68)80076-3.

[4] D. Dini, Y. Halpin, J.G. Vos, E.A. Gibson, The influence of the preparation method of NiO<inf>x</inf> photocathodes on the efficiency of p-type dye-sensitized solar cells, Coord. Chem. Rev. 304–305 (2015) 179–201. doi:10.1016/j.ccr.2015.03.020.

[5] D. Dini, Nanostructured Metal Oxide Thin Films as Photoactive Cathodes of P- Type Dye- Sensitised Solar Cells, Phys. Chem. Commun. 3 (2016) 14.

[6] A. Hagfeldt, G. Boschloo, L. Sun, L. Kloo, H. Pettersson, Dye-Sensitized Solar Cells, Chem. Rev. 110 (2010) 6595. doi:10.1021/cr900356p.

[7] M. Bonomo, D. Dini, Nanostructured p-type semiconductor electrodes and photoelectrochemistry of their

reduction processes, Energies. 9 (2016). doi:10.3390/en9050373.

[8] K. Kakiage, Y. Aoyama, T. Yano, K. Oya, J. Fujisawa, M. Hanaya, Highly-efficient dye-sensitized solar cells with collaborative sensitization by silyl-anchor and carboxy-anchor dyes, Chem. Commun. 51 (2015) 15894. doi:10.1039/C5CC06759F.

[9] I.R. Perera, T. Daeneke, S. Makuta, Z. Yu, Y. Tachibana, A. Mishra, et al., Application of the tris(acetylacetonato)iron(III)/(II) redox couple in p-type dye-sensitized solar cells, Angew. Chemie - Int. Ed. 54 (2015) 3758. doi:10.1002/anie.201409877.

[10] J. He, H. Lindström, A. Hagfeldt, S.-E. Lindquist, Dye-sensitized nanostructured tandem cell-first demonstrated cell with a dye-sensitized photocathode, Sol. Energy Mater. Sol. Cells. 62 (2000) 265. doi:http://dx.doi.org/10.1016/S0927-0248(99)00168-3.

[11] A. Nakasa, H. Usami, S. Sumikura, S. Hasegawa, T. Koyama, E. Suzuki, A high voltage dye-sensitized solar cell using a nanoporous NiO photocathode, Chem. Lett. 34 (2005) 500. doi:10.1246/cl.2005.500.

[12] A. Nattestad, I. Perera, L. Spiccia, Developments in and prospects for photocathodic and tandem dye-sensitized solar cells, J. Photochem. Photobiol. C Photochem. Rev. 28 (2016) 44–71. doi:10.1016/j.jphotochemrev.2016.06.003.

[13] M. Congiu, M.L. De Marco, M. Bonomo, D. Dini, C.F.O. Graeff, Solar cells, J. Nanoparticle Res. 19 (2017). http://hdl.handle.net/2060/19680022054.

[14] W. Shockley, H.J. Queisser, Detailed balance limit of efficiency of p-n junction solar cells, J. Appl. Phys. 32 (1961) 510. doi:10.1063/1.1736034.

[15] M. Awais, M. Rahman, J.M. Don MacElroy, D. Dini, J.G. Vos, D.P. Dowling, Application of a novel microwave plasma treatment for the sintering of nickel oxide coatings for use in dye-sensitized solar cells, Surf. Coatings Technol. 205 (2011) S245–S249. doi:10.1016/j.surfcoat.2011.01.020.

[16] G. Naponiello, I. Venditti, V. Zardetto, D. Saccone, A. Di Carlo, I. Fratoddi, et al., Photoelectrochemical characterization of squaraine-sensitized nickel oxide cathodes deposited via screen-printing for p-type dye-sensitized solar cells, Appl. Surf. Sci. 356 (2015) 911–920. doi:10.1016/j.apsusc.2015.08.171.

[17] E.A. Gibson, M. Awais, D. Dini, D.P. Dowling, M.T. Pryce, J.G. Vos, et al., Dye sensitised solar cells with nickel oxide photocathodes prepared via scalable microwave sintering., Pccp. 15 (2013) 2411–2420. doi:10.1039/c2cp43592f.

[18] M. Awais, E. Gibson, J.G. Vos, D.P. Dowling, A. Hagfeldt, D. Dini, Fabrication of Efficient NiO Photocathodes Prepared via RDS with Novel Routes of Substrate Processing for p-Type Dye-Sensitized Solar Cells, ChemElectroChem. 1 (2014) 384. doi:10.1002/celc.201300178.

[19] C.J. Wood, G.H. Summers, C.A. Clark, N. Kaeffer, M. Braeutigam, L.R. Carbone, et al., A comprehensive comparison of dye-sensitized NiO photocathodes for solar energy conversion., Phys. Chem. Chem. Phys. 18 (2016) 10727. doi:10.1039/c5cp05326a.

[20] F. Decker, The electrochromic process in non-soichiometric nickel oxide thin film electrodes, Electrochim. Acta. 37 (1992) 1033–1038. doi:http://dx.doi.org/10.1016/0013-4686(92)85220-F.

[21] S. Hüfner, Electronic structure of NiO and related 3d-transition-metal compounds, Adv. Phys. 43 (1994) 183–356. doi:10.1080/00018739400101495.

[22] M. Bonomo, A.G. Marrani, V. Novelli, M. Awais, D.P. Dowling, J.G. Vos, et al., Surface properties of nanostructured NiO undergoing electrochemical oxidation in 3-methoxy-propionitrile, Appl. Surf. Sci. 403 (2017) 441–447. doi:10.1016/j.apsusc.2017.01.202.

[23] M. Awais, D.D. Dowling, F. Decker, D. Dini, Photoelectrochemical properties of mesoporous NiO x deposited on technical FTO via nanopowder sintering in conventional and plasma atmospheres, Springerplus. 4 (2015) 564. doi:10.1186/s40064-015-1265-3.

[24] M. Awais, D.D. Dowling, M. Rahman, J.G. Vos, F. Decker, D. Dini, Spray-deposited NiO x films on ITO substrates as photoactive electrodes for p-type dye-sensitized solar cells, in: J. Appl. Electrochem., 2013: pp. 191–197. doi:10.1007/s10800-012-0506-1.

[25] J. He, H. Lindström, A. Hagfeldt, S.-E. Lindquist, Dye-Sensitized Nanostructured p-Type Nickel Oxide Film as a Photocathode for a Solar Cell, J. Phys. Chem. B. 103 (1999) 8940. doi:10.1021/jp991681r.

[26] F. Vera, R. Schrebler, E. Muñoz, C. Suarez, P. Cury, H. Gómez, et al., Preparation and characterization of Eosin B- and Erythrosin J-sensitized nanostructured NiO thin film photocathodes, Thin Solid Films. 490 (2005). doi:10.1016/j.tsf.2005.04.052.

[27] M. Bonomo, N. Barbero, F. Matteocci, A. Di Carlo, C. Barolo, D. Dini, Beneficial Effect of Electron-Withdrawing Groups on the Sensitizing Action of Squaraines for p-Type Dye-Sensitized Solar Cells, J. Phys. Chem. C. 120 (2016) 16340–16353. doi:10.1021/acs.jpcc.6b03965.

[28] A.G. Marrani, V. Novelli, S. Sheehan, D.P. Dowling, D. Dini, Probing the redox states at the surface of electroactive nanoporous nio thin films, ACS Appl. Mater. Interfaces. 6 (2014) 143–152. doi:10.1021/am403671h.

[29] J.H. Scofield, Hartree-Slater subshell photoionization cross-sections at 1254 and 1487 eV, J. Electron Spectros. Relat. Phenomena. 8 (1976) 129–137. doi:http://dx.doi.org/10.1016/0368-2048(76)80015-1.

[30] S. Sheehan, G. Naponiello, F. Odobel, D.P. Dowling, A. Di Carlo, D. Dini, Comparison of the photoelectrochemical properties of RDS NiO thin films for p-type DSCs with different organic and organometallic dye-sensitizers and evidence of a direct correlation between cell efficiency and charge recombination, J. Solid State Electrochem. 19 (2015) 975–986. doi:10.1007/s10008-014-2703-9.

[31] L. Nahon, A. Svensson, P. Morin, Experimental study of the 4d ionization continuum in atomic iodine by photoelectron and photoion spectroscopy, 43 (1991) 2328–2337.

[32] M. Arbman, S. Holmberg, M. Lundholm, H. Siegbahn, Liquid ESCA Measurements and ECP Calculations on the 3d Spectrum of I3−, Chem. Phys. 1 (1983) 113–119.

[33] P.M.A. Sherwood, X-Ray Photoelectron Spectroscopic Studies of Some Iodine Compounds, J. Chem. Soc. (1976) 1805–1820. doi:10.1039/F29767201805.

[34] S.K. Eriksson, I. Josefsson, N. Ottosson, G. Öhrwall, O. Björneholm, H. Siegbahn, et al., Solvent dependence of the electronic structure of I(-) and I3(-)., J. Phys. Chem. B. 118 (2014) 3164–74. doi:10.1021/jp500533n.

[35] I. Josefsson, S.K. Eriksson, N. Ottosson, G. Öhrwall, H. Siegbahn, A. Hagfeldt, et al., Collective hydrogen-bond dynamics dictates the electronic structure of aqueous I3(-)., Phys. Chem. Chem. Phys. 15 (2013) 20189–20196. doi:10.1039/c3cp52866a.

[36] M. Bonomo, D. Dini, A.G. Marrani, Adsorption Behavior of I3- and I- Ions at a Nanoporous NiO/Acetonitrile Interface Studied by X-ray Photoelectron Spectroscopy, Langmuir. 32 (2016) 11540–11550. doi:10.1021/acs.langmuir.6b03695.

[37] R. Weber, B. Winter, P.M. Schmidt, W. Widdra, I. V. Hertel, M. Dittmar, et al., Photoemission from Aqueous Alkali-Metal−Iodide Salt Solutions Using EUV Synchrotron Radiation, J. Phys. Chem. B. 108 (2004) 4729–4736. doi:10.1021/jp030776x.

[38] L. Partanen, M.H. Mikkelä, M. Huttula, M. Tchaplyguine, C. Zhang, T. Andersson, et al., Solvation at

nanoscale: Alkali-halides in water clusters, J. Chem. Phys. 138 (2013). doi:10.1063/1.4775586.

[39] N. Ottosson, J. Heyda, E. Wernersson, W. Pokapanich, S. Svensson, B. Winter, et al., The influence of concentration on the molecular surface structure of simple and mixed aqueous electrolytes., Phys. Chem. Chem. Phys. 12 (2010) 10693–700. doi:10.1039/c0cp00365d.

[40] B. Philippe, B.-W. Park, R. Lindblad, J. Oscarsson, S. Ahmadi, E.M.J. Johansson, et al., Chemical and Electronic Structure Characterization of Lead Halide Perovskites and Stability Behavior under Different Exposures - a Photoelectron Spectroscopy Investigation, Chem. Mater. 27 (2015) 1720–1731. doi:10.1021/acs.chemmater.5b00348.

[41] J.J. Chen, N. Winograd, The effects of preadsorbed CO on the chemistry of CH3 and CH3I on Pd{111}, Surf. Sci. 314 (1994) 188–200. doi:10.1016/0039-6028(94)90006-X.

[42] F.. R. Solymosi K, Spectroscopic study on the adsorption and dissociation of CH3I on Pd(100): thermal and photo effects, Surf. Sci. 280 (1993) 38–49.

[43] X.L. Zhou, F. Solymosi, P.M. Blass, K.C. Cannon, J.M. White, Interactions of methyl halides (Cl, Br and I) with Ag(111), Surf. Sci. 219 (1989) 294–316. doi:10.1016/0039-6028(89)90214-8.

[44] F. Zaera, H. Hoffmann, Detection of Chemisorbed Methyl and Methylene Groups: Surface Chemistry of Methyl Iodide on Pt(111), J. Phys. Chem. C. 95 (1991) 6297. doi:10.1021/j100169a042.

[45] R.J.T. and K.D.C. and G.W.C. and H.H. Wang, States determined by photoelectron spectroscopy in the perchlorate and perrhenate of TMTSF, J. Phys. C Solid State Phys. 18 (1985) 5501.

[46] V.I. Nefedov, Y.V. Salyn, G. Leonhardt, R. Scheibe, A comparison of different spectrometers and charge corrections used in X-ray photoelectron spectroscopy, J. Electron Spectros. Relat. Phenomena. 10 (1977) 121–124. doi:http://dx.doi.org/10.1016/0368-2048(77)85010-X.

[47] M. Awais, D.P. Dowling, M. Rahman, J.G. Vos, F. Decker, D. Dini, Spray-deposited NiOx films on ITO substrates as photoactive electrodes for p-type dyesensitized solar cells, J Appl Electrochem. 43 (2013). doi:10.1007/s10800-012-0506-1.

[48] M. Giustini, D. Angelone, M. Parente, D. Dini, F. Decker, A. Lanuti, et al., Emission spectra and transient photovoltage in dye-sensitized solar cells under stress tests, J. Appl. Electrochem. 43 (2013) 209–215. doi:10.1007/s10800-012-0484-3.

[49] G. Boschloo, A. Hagfeldt, Spectroelectrochemistry of nanostructured NiO, J. Phys. Chem. B. 105 (2001) 3039–3044. doi:10.1021/jp003499s.

[50] M.A. Van Veenendaal, G.A. Sawatzky, Nonlocal screening effects in 2p x-ray photoemission spectroscopy core-level line shapes of transition metal compounds, Phys. Rev. Lett. 70 (1993) 2459–2462. doi:10.1103/PhysRevLett.70.2459.

[51] L. Soriano, I. Preda, A. Gutiérrez, S. Palacín, M. Abbate, A. Vollmer, Surface effects in the Ni 2p x-ray photoemission spectra of NiO, Phys. Rev. B - Condens. Matter Mater. Phys. 75 (2007) 1–4. doi:10.1103/PhysRevB.75.233417.

[52] D. Alders, F. Voogt, T. Hibma, G.A. Sawatzky, Nonlocal screening effects in 2p x-ray photoemission spectroscopy of NiO (100), Phys. Rev. B. 54 (1996) 7716–7719. doi:10.1103/PhysRevB.54.7716.

[53] R.J.O. Mossanek, I. Preda, M. Abbate, J. Rubio-Zuazo, G.R. Castro, A. Vollmer, et al., Investigation of surface and non-local screening effects in the Ni 2p core level photoemission spectra of NiO, Chem. Phys. Lett. 501 (2011) 437–441. doi:10.1016/j.cplett.2010.11.050.

[54] J. Van Elp, H. Eskes, P. Kuiper, G.A. Sawatzky, Electronic structure of Li-doped NiO, Phys. Rev. B. 45 (1992)

1612–1622. doi:10.1103/PhysRevB.45.1612.

[55] I. Preda, R.J.O. Mossanek, M. Abbate, L. Alvarez, J. Méndez, A. Gutiérrez, et al., Surface contributions to the XPS spectra of nanostructured NiO deposited on HOPG, Surf. Sci. 606 (2012) 1426–1430. doi:10.1016/j.susc.2012.05.005.

[56] V. Biju, M. Abdul Khadar, Electronic structure of nanostructured nickel oxide using Ni 2p XPS analysis, J. Nanoparticle Res. 4 (2002) 247–253. doi:10.1023/A:1019949805751.

[57] M.A. Peck, M.A. Langell, Comparison of nanoscaled and bulk NiO structural and environmental characteristics by XRD, XAFS, and XPS, Chem. Mater. 24 (2012) 4483–4490. doi:10.1021/cm300739y.

[58] S. D'Addato, V. Grillo, S. Altieri, R. Tondi, S. Valeri, S. Frabboni, Structure and stability of nickel/nickel oxide core–shell nanoparticles, J. Phys. Condens. Matter. 23 (2011) 175003. doi:10.1088/0953-8984/23/17/175003.

[59] G. Tyuliev, M. Sokolova, Temperature dependence of Ni3+ quantity in the surface layer of NiO, Appl. Surf. Sci. 52 (1991) 343–349. doi:10.1016/0169-4332(91)90078-X.

[60] B.P. Payne, M.C. Biesinger, N.S. McIntyre, The study of polycrystalline nickel metal oxidation by water vapour, J. Electron Spectros. Relat. Phenomena. 175 (2009) 55–65. doi:10.1016/j.elspec.2009.07.006.

[61] P. Kuiper, G. Kruizinga, J. Ghijsen, G.A. Sawatzky, H. Verweij, Character of Holes in ${\mathrm{Li}}_{x}{\mathrm{Ni}}_{1-x}\mathrm{O}$ and Their Magnetic Behavior, Phys. Rev. Lett. 62 (1989) 221–224.

[62] A.P. Grosvenor, M.C. Biesinger, R.S.C. Smart, N.S. McIntyre, New interpretations of XPS spectra of nickel metal and oxides, Surf. Sci. 600 (2006) 1771–1779. doi:10.1016/j.susc.2006.01.041.

Captions

Figure 1. Top: effect of the continuous cycling of the potential (E) on the voltammogram of EryB sensitized NiO (scan rate: 10 mV s^{-1}). The applied potential values are referred to the reference couple Ag/AgCl. Bottom: Comparison of the first and 50^{th} voltammetric cycles of EryB sensitized NiO. The two differently coloured curves have been selected from the figure on the top.

Figure 2. Top: Chronoamperometric curve of EryB sensitized NiO when the electrode is polarized at E = 0.9 V *vs* Ag/AgCl, i.e. at the potential corresponding to the completion of the first step of NiO oxidation (Figure 1). The sample obtained at the end of this potentiostatic step is denominated **ox**. Bottom: Chronoamperometric curve of EryB sensitized NiO when the electrode is polarized at E = -0.27 V V *vs* Ag/AgCl, i.e. at the potential corresponding to the full neutralization of NiO (Figure 1). The sample obtained at the end of this potentiostatic step is denominated **red**.

Figure 3. I 4d XPS ionization region. Experimental points are represented in dots, while results of fitting reconstruction are reported in solid lines. Samples from top to bottom: **graphite** (a), **pristine** (b), **red** (c), **ox** (d), **CV1** (e), **CV25** (f) and **CV50** (g) (see Experimental Section for details).

Figure 4. I 3d XPS ionization region. Experimental points are represented in dots, while results of fitting reconstruction are reported in solid lines. Samples from top to bottom: **graphite** (a), **pristine** (b), **red** (c), **ox** (d), **CV1** (e), **CV25** (f) and **CV50** (g) (see Experimental Section for details).

Figure 5. Cl 2p XPS ionization region of sample **ox**. Experimental points are represented in dots, while results of fitting reconstruction are reported in solid lines. Color key for 3/2 spin−orbit components: ClO_4^- (red), ClO_3^- (green), Cl^- (blue). Top (a): spectra acquired at t = 0; bottom (b): spectra acquired at t = 1 h.

Figure 6. XPS survey spectrum of **pristine** sample. Inset: high-resolution Ni 2p region.

Figure 1

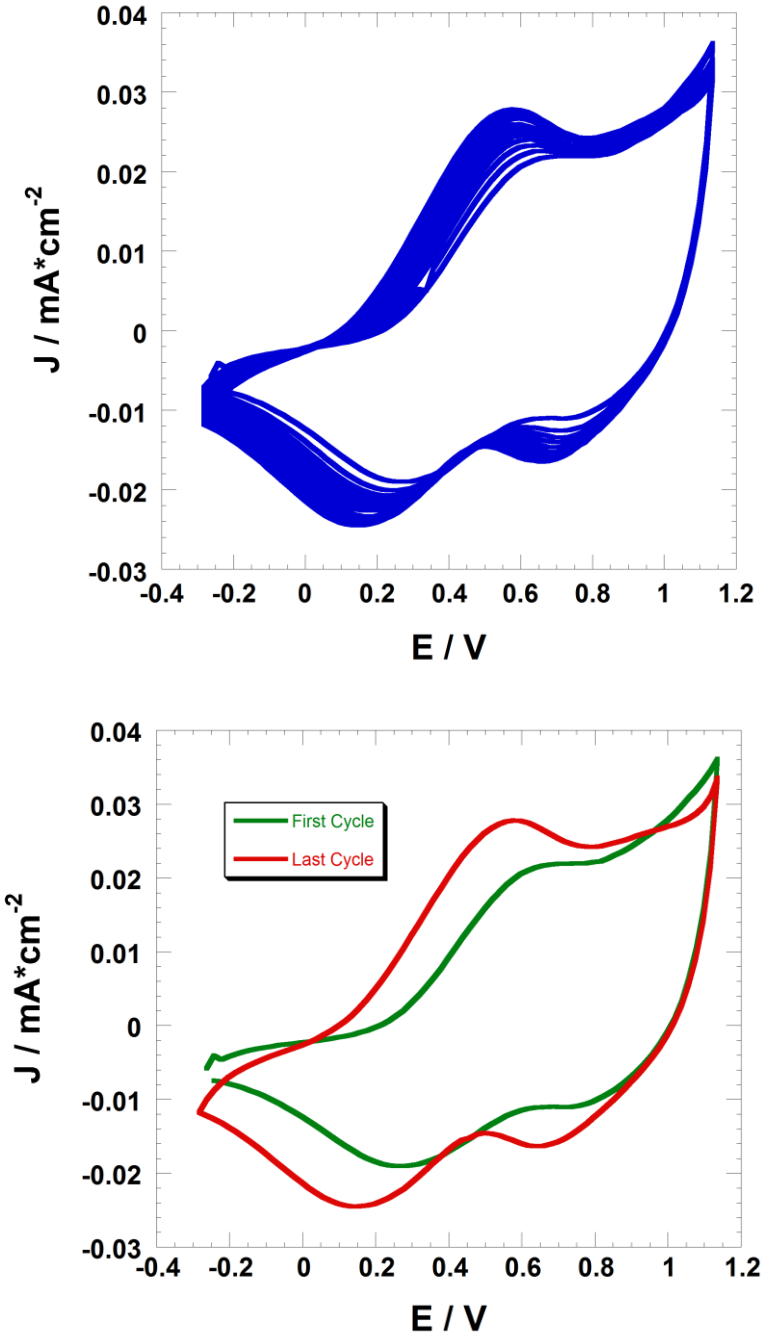
0.04
0.03
0.02
0.01
0
-0.01
-0.02
-0.03
J / mA*cm-2
-0.4
-0.2
0
0.2
0.4
0.6
0.8
1
1.2
E / V
First Cycle
Last Cycle

Figure 2

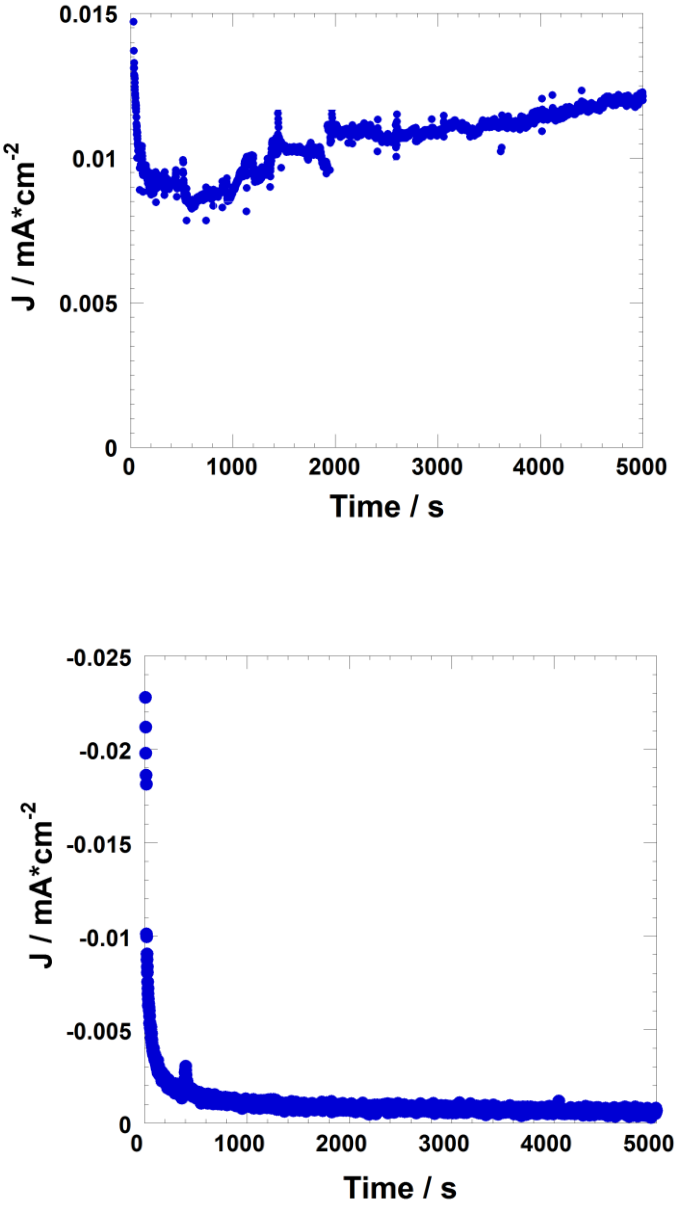
0.015
0.01
0.005
0
J / mA*cm-2
0
1000
2000
3000
4000
5000
Time / s
-0.025
-0.02
-0.015
-0.01
-0.005
0
J / mA*cm-2
0
1000
2000
3000
4000
5000
Time / s

Figure 3

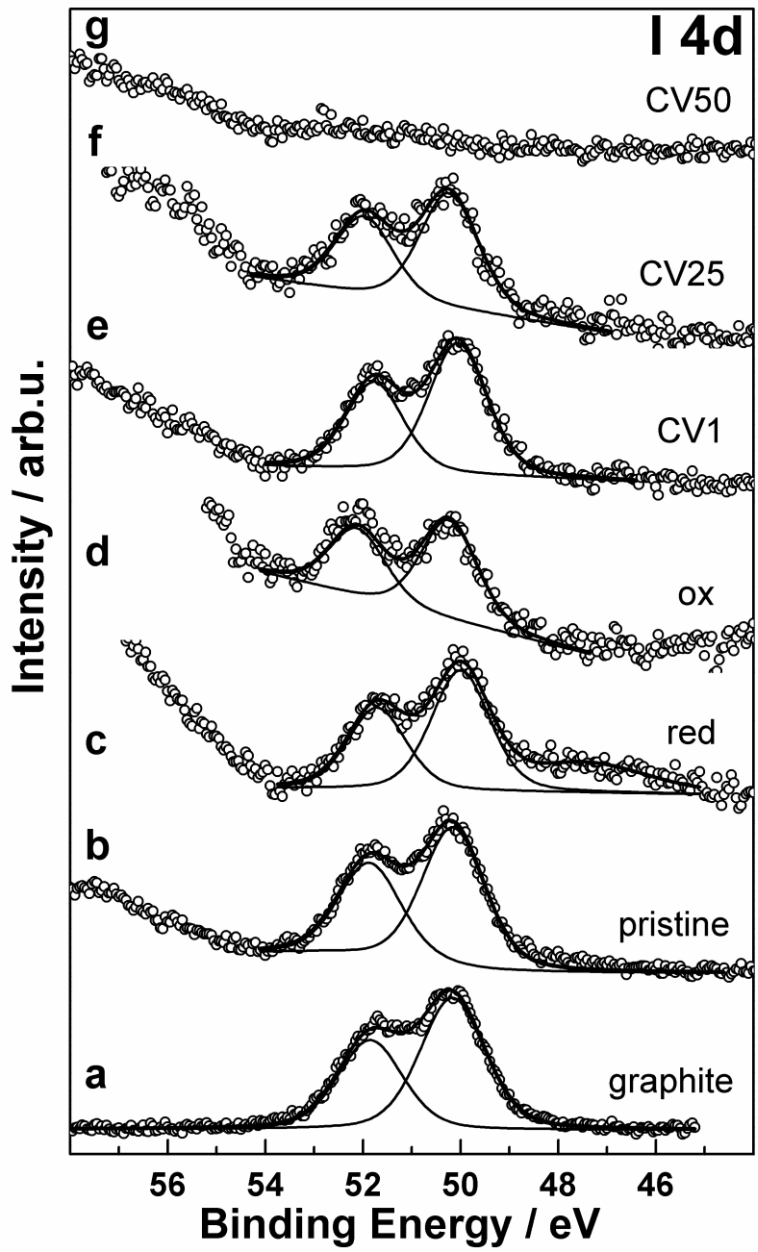
g
I 4d
CV50
f
CV25
e
CV1
d
ox
c
red
b
pristine
a
graphite
Intensity / arb.u.
56
54
52
50
48
46
Binding Energy / eV

Figure 4

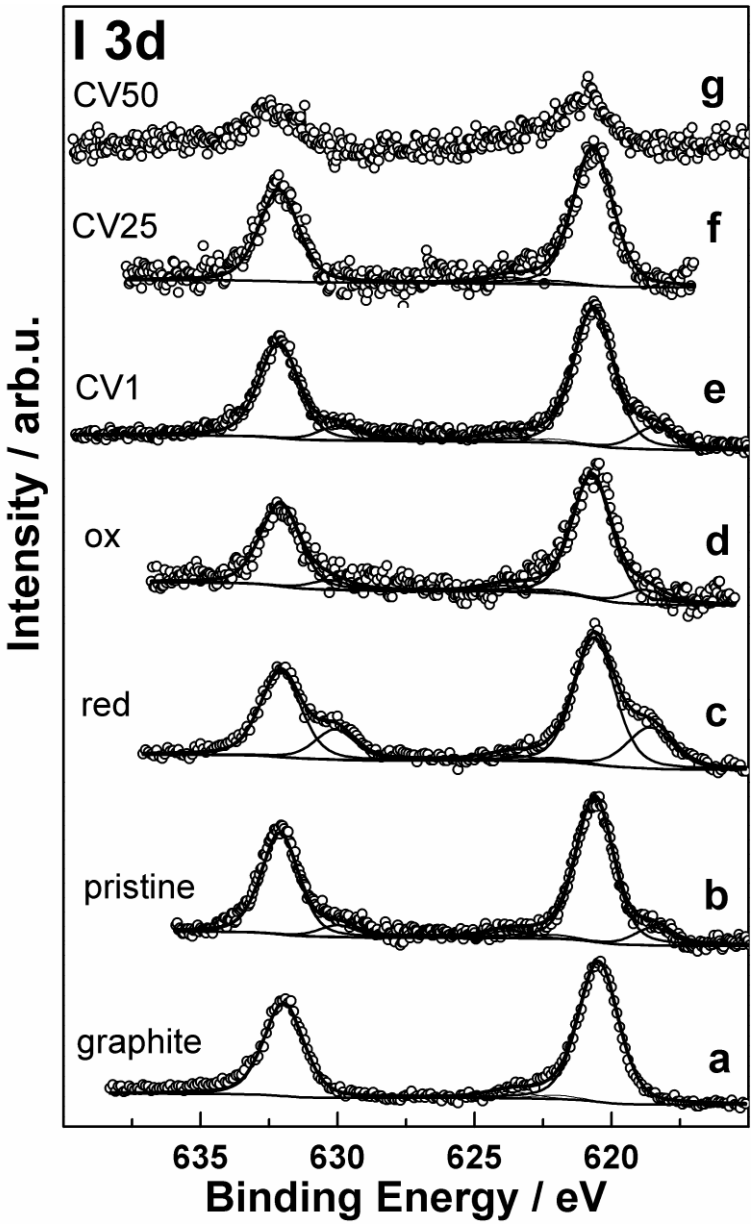
I 3d
CV50
g
CV25
f
CV1
e
ox
d
red
c
pristine
b
graphite
a
Intensity / arb.u.
635
630
625
620
Binding Energy / eV

Figure 5

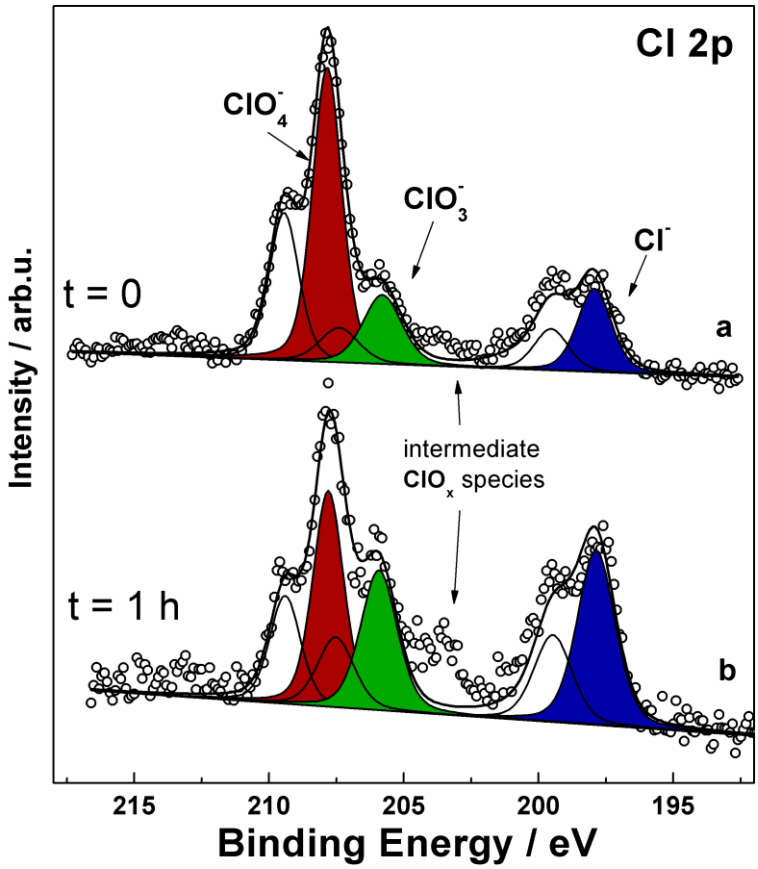
Cl 2p
ClO4-
ClO3-
Cl-
t = 0
a
intermediate
ClOx species
t = 1 h
b
Intensity / arb.u.
215
210
205
200
195
Binding Energy / eV

Figure 6

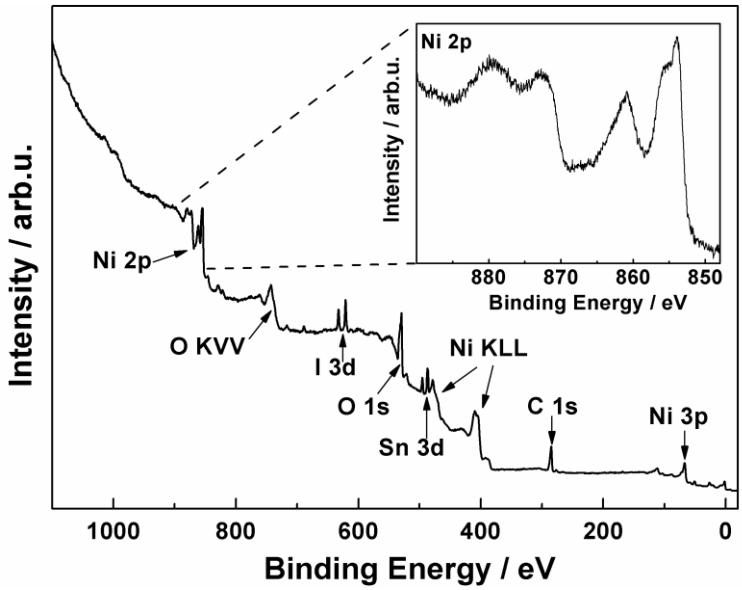

Tables

Table 1. Quantitative area ratios between relevant XPS peaks for all the samples investigated.

	pristine	**red**	**ox**	**CV1**	**CV25**	**CV50**
I $3d_{5/2}$/Ni $2p_{3/2}$	0.116	0.031	0.025	0.055	0.037	n.d.
Cl 2p/Ni $2p_{3/2}$	0.064[a]	0.034	0.441	0.061	0.727	0.360

[a] Immersed in the electrolytic solution for 1 min

TOC graphics

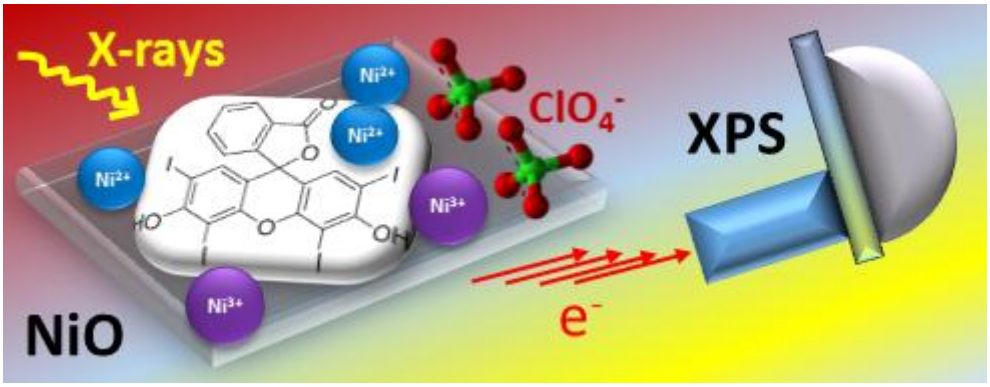

X-ray photoelectron spectroscopy investigation of nanoporous NiO electrodes sensitized with Erythrosine B

Matteo Bonomo, Danilo Dini, Andrea Giacomo Marrani*, Robertino Zanoni

Department of Chemistry, University of Rome "La Sapienza", P.le Aldo Moro 5, 00185 Rome, Italy

*Corresponding author. Tel.: +39 06 4991 3344; fax: +39 06 49913175.

E-mail address: andrea.marrani@uniroma1.it

Abstract

Nanoporous NiO thin films were prepared onto FTO glass substrates by means of screen-printing and were sensitized with Erythrosin B (EryB) dye. The obtained material was electrochemically treated and characterized with *ex-situ* X-ray photoelectron spectroscopy in order to gain information beneficial to the application of sensitized NiO as photocathodes of *p*-type dye-sensitised solar cells (*p*-DSCs). In particular, EryB-sensitised NiO films underwent a series of electrochemical treatments in $LiClO_4$/Acetonitrile (ACN) electrolyte devised so as to simulate possible conditions the electrode might encounter during operation in the photoelectrochemical cell. Upon potential-cycling in a range where the two NiO faradic events Ni(II)→Ni(III) and Ni(III)→Ni(IV) occur, X-ray photoelectron spectroscopy revealed that Erythrosin B dye experiences a partial detachment from the NiO surface. This detachment seems to be paralleled by the formation of stable $(Ni)^{+}(ClO_4)^{-}$ couples. Overall, the EryB dye displayed an acceptable electrochemical stability onto the surface of NiO electrode up to 50 cyclic voltammetries in the range -0.27 ÷ +1.13 V vs. Ag/AgCl. These results are useful for the evaluation of electrochemical stability of the dye when the this is immobilised onto an electrode surface and are beneficial for a better comprehension of the degradation phenomena operating in real photoconversion device.